

Analyzing OH*, CH*, and C2* chemiluminescence of bifurcating FREI propane-air flames in a micro flow reactor

Marc E. Baumgardner^{a,*}, John Harvey^a

^a*Mechanical Engineering Department, Gonzaga University, 502 E. Boone Ave, Spokane, WA 99258, USA*

Abstract

An experimental investigation of spontaneous flame chemiluminescence of OH*, CH*, and C2* radicals was conducted for premixed propane-air flames in a micro flow reactor. Equivalence ratios from 0.7 to 1.4 were examined and correlated well to the ratio of OH*/CH* and C2*/CH* ($R^2 > 0.999$ for C2*/CH* power fit). The OH*/CH* ratio better correlated with equivalence ratio for lean flames, while the C2*/CH* ratio better correlated with rich flames. The equivalence ratio model was used to calculate the axial local equivalence ratio for a rich propane-air flame (ϕ of 1.5) exhibiting strong bifurcating FREI behavior, resulting in three visible flame fronts. The measured intensities of OH*, CH*, and C2* chemiluminescence, as well as the calculated local equivalence ratio along the reactor axis support the numerical model explanations of the observed bifurcating FREI flames available in the literature. This work highlights the novel application of this diagnostic technique in the context of micro flow reactors.

*Corresponding author: baumgardner@gonzaga.edu

1. Introduction

Recently, Alipoor and Mazaheri examined bifurcating hydrogen flames experiencing repetitive extinction and ignition (FREI) in a heated micro channel[1]. Earlier numerical analysis by Nakamura et al.[2] examined similar behavior for methane-air FREI flames in a micro flow reactor (MFR). These works predicted that primary fuel species were consumed by the most upstream flame front, leaving downstream flames to burn progressively leaner with respect to the partially combusted fuel fragments. To further validate this numerical work, additional experimental analysis is required to examine the axial species profiles in such bifurcating flames.

The passive collection of spontaneous flame chemiluminescence of excited state radicals can offer an inexpensive, relatively straightforward approach to collecting such axial profiles in MFRs. Furthermore, it is well-documented that the ratio of OH^*/CH^* and C_2^*/CH^* can be directly correlated to air-fuel equivalence ratio (ϕ) within the flame[3–5]. One challenge with such flame spectroscopy is the line-of-sight nature of the observation. The typical MFR, however, is perfectly situated for a simple optical setup to collect light from within the reactor. Optical accessibility of the entire flame region is possible; both weak and strong flames are stable indefinitely; and the periodic nature of most FREI flames enables examination of a naturally transient processes. Herein this simple diagnostic is used, for the first time in an MFR, to examine the behavior of propane-air flames for a variety of equivalence ratios. More specifically, the ratios of OH^*/CH^* and C_2^*/CH^* are used to infer the local flame equivalence ratio for stable flames; that model is then applied to a rich propane-air FREI flame exhibiting strong bifurcations to examine the axial

change in the local equivalence ratio along the length of the MFR.

2. Experimental methods

The MFR used herein is a 2.3 mm diameter quartz reactor, situated above a flat flame burner fueled with a hydrogen-air mixture. Premixed air and fuel enters the reactor upstream of the burner location and is then subjected to the increasing temperature profile of the reactor as it extends above the burner. A detailed description of the MFR and the optical diagnostics (i.e., components, layout, calibration, resolution, etc.) is available in the Supplementary Material.

The collection optics consists of a 2-in diameter biconvex lens ($f = 60$ mm)—the short focal length maximizes light collection from within the MFR. The collected light is focused on to a fiber optic cable coupled to a UV-Vis spectrometer (Ocean Optics Jaz) with an effective range of 200 to 1100 nm. The lens arrangement is mounted on a translation stage parallel to the reactor, allowing full scans of the reaction zone at step-sizes as low as 0.2 mm. Additionally, a Nikon[®] D3300 digital camera with a 100 mm F2.8 Macro Rokinon[®] lens was used to capture traditional images of the MFR flames. A narrow bandpass filter centered at 431.4 ± 2.6 nm (FWHM 5 ± 1 nm) enabled visual observation of the CH* emission.

An example spectra of a typical propane-air flame is provided in the Supplementary Material. The major OH*, CH*, and C2* emission bands were observed near 309 nm, 431 nm, and 516 nm, respectively. The spectra displayed some broad non-linear background emission, primarily attributable to CO2* [6, 7], which was subtracted from the signal to yield the final result.

Careful consideration should be given to exact spectral bands considered for these measurements – more detail is provided in the Supplementary Material.

3. Results and discussion

We first examined strong, stable flames at 40 cm/s and equivalence ratios of 0.7 to 1.4. This velocity was selected because the flames trip into FREI at lower values; alternatively, higher velocities push the flame too far over the burner resulting in background water emission from the hydrogen flame overwhelming the spectral signal from the MFR. Example axial species profiles for three stable flames at equivalence ratios of 0.7, 1.0, and 1.3 are provided in the Supplementary Material.

For each equivalence ratio, the location of maximum signal intensity was recorded. Once the baseline was subtracted, the peak value for both OH* and C2* were normalized to the CH* signal and correlated against the nominal inlet equivalence ratio (see Fig. 1). Equivalence ratio tracked well with both of the ratios examined though the OH*/CH* ratio was more sensitive at leaner equivalence ratios, while the C2*/CH* better correlated for richer mixtures. A simple power curve fit, $R^2 > 0.999$, as recommended by Cheng et al.[8] was applied (Fig. 1) and extrapolated to ϕ of 1.5, which corresponds to the conditions of the bifurcating flame examined. It is also worth mentioning that previous studies[5] have demonstrated such correlations for propane flames are valid up to a ϕ of about 1.6, but lose sensitivity beyond this point.

Figure 2a background displays a photo of the bifurcated flame taken with the digital camera while Fig. 2b background displays the same flame but viewed through a CH* filter. The foreground in Fig. 2b is the vertically

binned pixel intensity, which gives a proxy for the spatial intensity of the CH^* profile. Figure 2c shows the axial profiles of the OH^* , CH^* , and C_2^* values taken with the spectrometer. The OH^* intensity is shown at 5x to make it more visible in the figure. The ratio of the absolute C_2^*/CH^* intensities shown was used to calculate the local equivalence ratio according to the model from Fig. 1; this calculated local equivalence ratio is provided in Fig. 2a overlaid on top of the actual bifurcated flame image to highlight how the equivalence ratio changes across each flame.

Numerical studies[1, 2] predict that the primary fuel species (i.e., propane here) is consumed across the first flame leaving partially combusted fuel fragments to be reacted in the downstream bifurcated flames. Thus, downstream flames should get progressively leaner until the original ignition location is reached, where two flames were initially formed. The main flame progresses upstream, subsequently bifurcating due to the influence of the wall temperature[1]. The second flame is much weaker and slowly progresses downstream consuming the available amount of fuel/air that existed at the moment of ignition, thus this latter flame should have an equivalence ratio approximately equal to that of the fresh mixture. Overall the calculated local equivalence ratio (Fig. 2a) tracks well with the observable bifurcated flames and strongly, albeit qualitatively, matches the numerical results available in the literature.

4. Conclusions

The absolute intensities of OH^* , CH^* , and C_2^* , and the C_2^*/CH^* -based equivalence ratio prediction were found to support numerical examinations

of bifurcating FREI flames available in the literature. These results highlight the novel application of this diagnostic technique to MFRs and further suggest this method can lend experimental evidence to numerical studies. Furthermore, this approach has advantages such as cost and ease of implementation as compared to alternatives such as LIF, high-speed ICCD cameras, or even sampling via micro-injection syringes and so could be incorporated with such techniques to provide a more comprehensive picture of the combustion in MFRs.

Acknowledgments

We would like to thank Robert and Claire McDonald, whose generosity has helped so many undergraduate students get involved in scientific research. This research did not receive any specific grant from funding agencies in the public, commercial, or not-for-profit sectors.

References

- [1] A. Alipoor, K. Mazaheri, Combustion characteristics and flame bifurcation in repetitive extinction-ignition dynamics for premixed hydrogen-air combustion in a heated micro channel, *Energy* 109 (2016) 650–663.
- [2] H. Nakamura, A. Fan, S. Minaev, E. Sereshchenko, R. Fursenko, Y. Tsuboi, K. Maruta, Bifurcations and negative propagation speeds of methane/air premixed flames with repetitive extinction and ignition in a heated microchannel, *Combustion and Flame* 159 (4) (2012) 1631–1643.

- [3] J. Kojima, Y. Ikeda, T. Nakajima, Basic aspects of OH(A), CH(A), and C2(d) chemiluminescence in the reaction zone of laminar methane-air premixed flames, *Combustion and Flame* 140 (1-2) (2005) 34–45.
- [4] S. Kim, C. Lee, M. Kwon, Measurement of Equivalence Ratio Using Optical Flame Chemiluminescence Sensor of Turbulent Diffusion Flame, *International Journal of Electrical Energy* 3 (3) (2015) 203–208.
- [5] J. Reyes, R. Kumar Abhinavam Kailasanathan, K. Ahmed, Relationship between the Chemiluminescence Intensity Ratio of C2* and CH*, Charge Pressure, and Equivalence Ratio for Gasoline, *Energy and Fuels* 32 (10) (2018) 10933–10940.
- [6] M. M. Tripathi, S. R. Krishnan, K. K. Srinivasan, F. Y. Yueh, J. P. Singh, Chemiluminescence-based multivariate sensing of local equivalence ratios in premixed atmospheric methane-air flames, *Fuel* 93 (2012) 684–691.
- [7] T. F. Guiberti, D. Durox, T. Schuller, Flame chemiluminescence from CO₂- and N₂-diluted laminar CH₄/air premixed flames, *Combustion and Flame* 181 (2017) 110–122.
- [8] T. S. Cheng, C. Y. Wu, Y. H. Li, Y. C. Chao, Chemiluminescence measurements of local equivalence ratio in a partially premixed flame, *Combustion Science and Technology* 178 (10-11) (2006) 1821–1841.

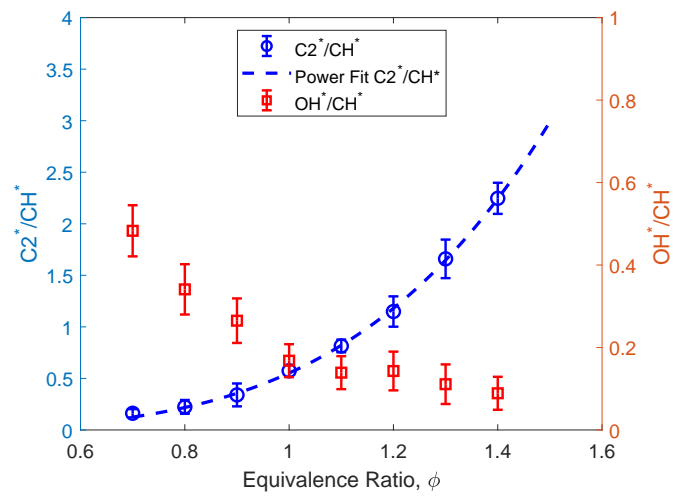


Figure 1: Comparison of OH^*/CH^* (squares) and C_2^*/CH^* (circles) as they relate to equivalence ratio. Also shown is a power law fit ($R^2 > 0.999$) of the C_2^*/CH^* data extrapolated up through ϕ of 1.5.

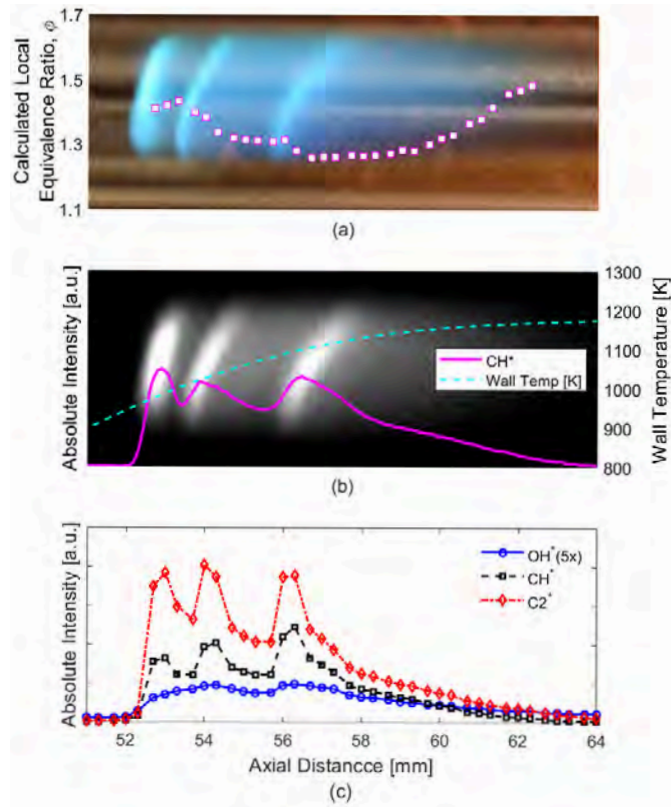


Figure 2: Photos and spectral profiles for propane-air flame at MFR inlet conditions of ϕ of 1.5 and 40 cm/s: (a) local equivalence ratio calculated from the C_2^*/CH^* ratio overlaid on a photo of the bifurcated flame; (b) photo taken with a CH^* filter, the corresponding vertically summed pixel intensity, and the reactor wall temperature; (c) absolute intensity profiles of OH^* , CH^* , and C_2^* . Note the OH^* intensity is shown at 5x to make it more visible.

Appendix A. Supplemental Material

The discussion below offers a more in-depth description of the micro flow reactor (MFR) experiment as well details on data taken to support the development of the model for equivalence ratio (ϕ) vs. OH^*/CH^* and C_2^*/CH^* ratios.

A schematic and photo of the micro flow reactor can be seen in Fig. A.1. The overall layout is very similar to that originally developed by Maruta et al.[1], though this incarnation has additional optical diagnostics added as detailed below. Mass flow controllers (Omega FMA5500 series) for air and propane control the fuel flow rates within $\pm 1\%$ of the desired value. After the mass flow controllers, the gases flow through one way check-valves to a mixing chamber and flashback arrestor before entering the MFR. The premixed propane-air mixture then flows through a 2.3 mm diameter quartz reactor (i.e., the MFR), which is situated above a McKenna-style flat flame burner (Holthuis & Associates) that is fueled with a hydrogen-air mixture. Hydrogen is used to fuel the burner so that the burner flame does not interfere with the CH^* chemiluminescence from the MFR.

The collection optics consists of a 2-in diameter biconvex lens with a focal length of 60 mm—the short focal length was chosen in order to collect as much light as possible from within the MFR focal volume. The collected light is then collimated via a 1/2-in diameter -20 mm lens and then focused down through a set of focusing optics (Ocean Optics 74-UV) on to a 1-m long, 400 μm core diameter fiber optic cable (Ocean Optics P400-1-SR). The fiber is coupled to a UV-Vis spectrometer (Ocean Optics Jaz) with an effective range of 200 to 1100 nm. The lens arrangement is mounted on a translation

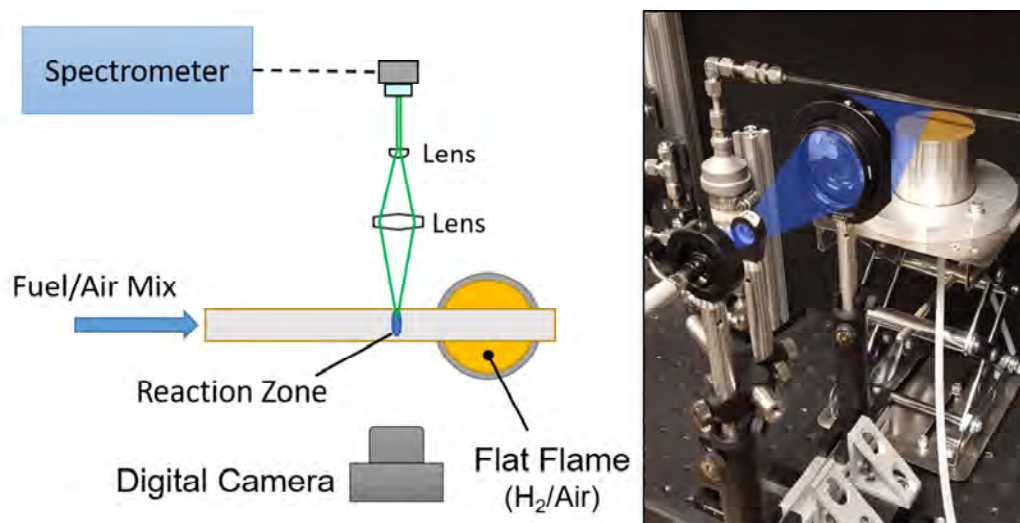


Figure A.1: Experimental setup showing MFR and collection optics: schematic at left and photo at right. The lens pair focuses light from the center of the MFR onto the fiber optic connected to the spectrometer. Note that the light collection path is highlighted in blue in the photo.

stage allowing full scans of the reaction zone. To assess the resolution of the system, ray-tracing software (Zemax) was used to determine that the minimum translation necessary to distinguish two neighboring points was approximately 0.2 mm. As a result, we chose to collect data at intervals of 0.3-0.4 mm to ensure the subsequent measurements were safely within the spatial resolution limits of the system. Therefore, the resolution seen in the manuscript (Fig. 2) represents very nearly the maximum resolution, i.e., minimum safe distance between data points possible, for the current setup. Further refinement of the optical system resolution would likely require the use of further apertures, a smaller diameter fiber, and a more finely graduated linear translation stage.

In addition to the spectrometer measurements, a Nikon[®] D3300 digital camera with a 100 mm F2.8 Macro Rokinon[®] lens was used to capture

traditional images of the MFR flames. Additionally, the same camera setup was used in conjunction with a narrow bandpass filter (Omega Optical Filters) centered at 431.4 ± 2.6 nm (FWHM 5 ± 1 nm) to visually observe the CH^* emission.

Figure A.2 shows an example spectra of a typical propane-air flame. The major OH^* , CH^* , and C_2^* emission bands are observed near 309 nm, 431 nm, and 516 nm, respectively. Note that in addition to the major $\text{C}_2^*(0,0)$ band near 516 nm the $\text{C}_2^*(1,0)$ band is also prominently visible near 470 nm. Following the advice of Kojima et al.[2], we integrated across the $\text{C}_2^*(0,0)$ band (which technically also included signal from the (1,1) peak near 513 nm) to obtain the C_2^* signal – this issue is discussed further below.

The spectra display some broad non-linear background emission, which has been shown to be primarily attributable to CO_2^* emission[3, 4]. This background CO_2^* was strongly correlated to equivalence ratio and had to be stripped out of the measurement before the true OH^* , CH^* , and C_2^* peaks could be measured. Figure A.2 shows the corresponding calculated baseline (black dashed line) which was subtracted from the spectral signal to yield the final result.

Using the arrangement depicted in Fig. A.1, we first examined the spectra of strong, stable flames for a variety of equivalence ratios at multiple velocities—for these flames, the nominal equivalence ratio was based off of the mass flow rates of air and fuel to the MFR inlet. Nominal equivalence ratios from 0.7 to 1.4 were examined at both 40 cm/s and 50 cm/s since flames at different velocities stabilize at different reactor wall temperatures. There were no observable differences in the spectral ratios measured between the

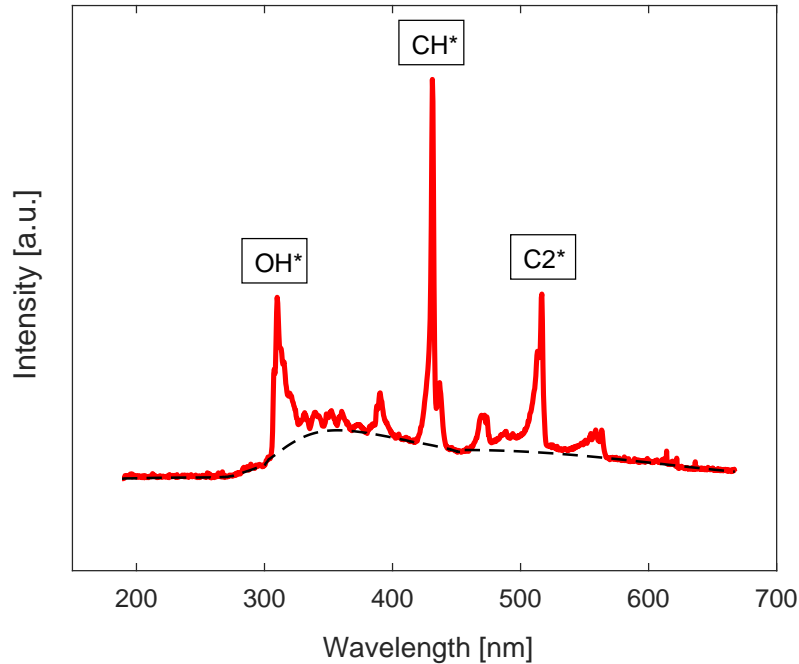


Figure A.2: An example flame spectra taken from the center of a stable, propane/air flame in the MFR; the spectra (solid red line) highlights the locations of the primary OH*, CH*, and C2* peaks. The corresponding baseline value for the spectra is the dashed black line.

two velocities, which makes sense given the flame temperature is considerably higher than the wall temperature[5] and thus dominates. This velocity range was also selected because the flames trip into FREI region at lower velocities; alternatively, higher velocities can push the flame too far over the flat flame burner resulting in background water emission from the hydrogen burner flame overwhelming the spectral signal from the MFR.

Spectral profiles for three nominal inlet equivalence ratios (0.7, 1.0, and 1.3) are shown in Fig. A.3. Here, the left axis indicates the absolute signal intensity in arbitrary units, while the right axis shows the calculated local equivalence ratio based off of the chemiluminescent ratios—OH*/CH* for ϕ

of 0.7, and $C2^*/CH^*$ for ϕ of 1.0 and 1.3. The basis for this calculation is discussed in the main paper and briefly below. The location of these flames stabilize at different values, with the ϕ of 1.0 flame stabilizing at the lowest reactor wall temperature (i.e., furthest upstream) followed by ϕ 1.3, and 0.7, respectively. This behavior corresponds to the relative flame speeds of each fuel and similar results were shown by DiStazio et al. for methane flames[6].

For each equivalence ratio (i.e., 0.7 through 1.4), the location of maximum signal intensity was found and the signal recorded—see example spectra in Fig. A.2. Once the baseline was subtracted, the peak value for both OH^* and $C2^*$ were normalized to the CH^* signal and correlated against the inlet nominal equivalence ratio (i.e., the value based off the mass flow measurements of air and fuel). Similar to other studies[2, 7], no appreciable difference was observed whether the peak signal intensity or the integrated signal around a given peak was used when examining the ratios of OH^*/CH^* or $C2^*/CH^*$. Furthermore, to maintain consistency with previous studies[2, 8, 9], only the signal integrated across the main peaks was used; specifically for $C2^*$, this meant examining only the $C2^*(0,0)$ band near 516 nm. The full data set across all the equivalence ratios examined (i.e., 0.7 to 1.4) are compiled in Fig. 1 in the main paper.

As validation of the setup and calibration data taken herein, the $C2^*/CH^*$ intensity ratios for the stable MFR propane flames across the range of equivalence ratios were compared against an array of methane and propane flame data from the literature. The results of this comparison are shown in Fig. A.4, and demonstrate the good agreement of the present work with previous studies. It is especially important to note the difference in behavior

between methane and propane flames. Whereas the relationship between the C_2^*/CH^* intensity ratio versus equivalence ratio caps about around a ϕ of 1.35 for methane, this relationship for propane is valid up to about a ϕ of 1.6 where it begins to lose sensitivity.

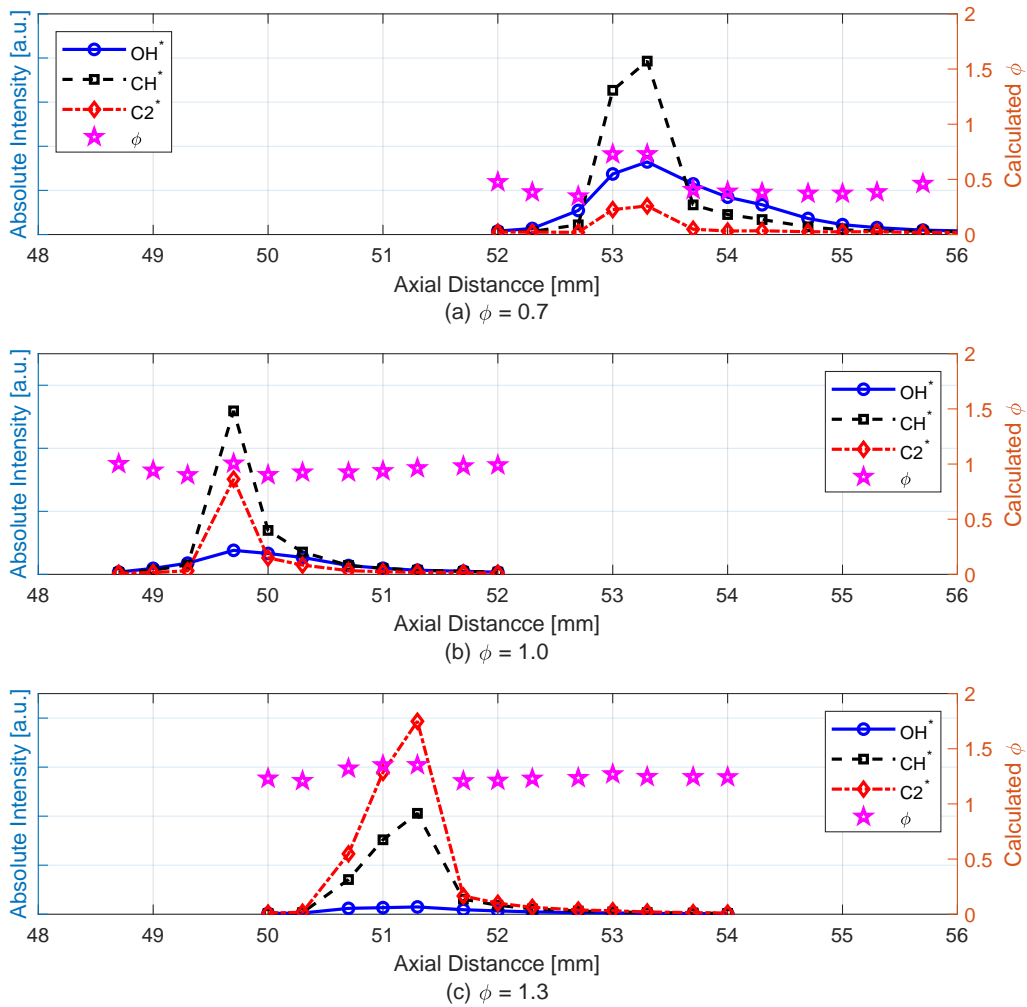


Figure A.3: Spectral profiles for strong stable propane-air flames at multiple bulk flow equivalence ratios and 40 cm/s: (a) ϕ of 0.7; (b) ϕ of 1.0; (c) ϕ of 1.3. Also shown on the right axis are the calculated local equivalence ratios based on the chemiluminescent ratios: OH^*/CH^* for ϕ of 0.7, and $\text{C2}^*/\text{CH}^*$ for ϕ of 1.0 and 1.3.

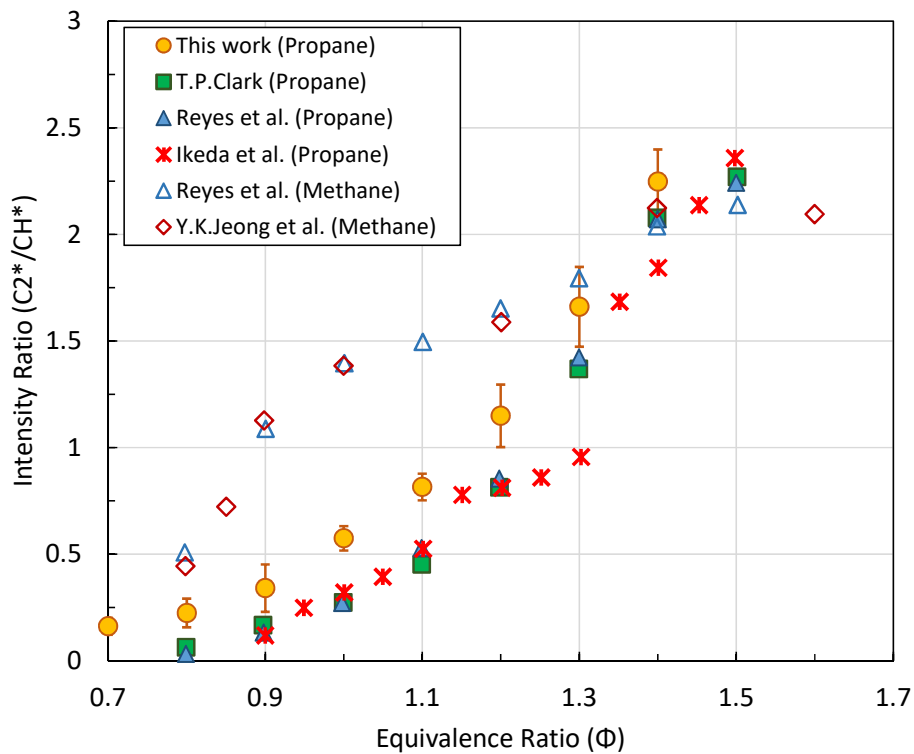


Figure A.4: Intensity ratio of $C2^*/CH^*$ for this work compared to several other studies for both propane and methane flames. Data from this work (i.e., propane) are filled orange circles; propane data adapted from Reyes et al.[10] are filled blue triangles, methane data are open blue triangles; propane data from T.P. Clark[11] are filled green squares; propane data from Ikeda et al.[12] are red asterisks; methane data from Y.K. Jeong et al.[13] are open red diamonds.

References

- [1] K. Maruta, T. Kataoka, N. Il, S. Minaev, R. Fursenko, Characteristics of combustion in a narrow channel with a temperature gradient, *Proceedings of the Combustion Institute* 30 (2) (2005) 2429–2436.
- [2] J. Kojima, Y. Ikeda, T. Nakajima, Spatially resolved measurement of OH*, CH*, and C*₂ chemiluminescence in the reaction zone of laminar methane/air premixed flames, *Proceedings of the Combustion Institute* 28 (2) (2000) 1757–1764.
- [3] M. M. Tripathi, S. R. Krishnan, K. K. Srinivasan, F. Y. Yueh, J. P. Singh, Chemiluminescence-based multivariate sensing of local equivalence ratios in premixed atmospheric methane-air flames, *Fuel* 93 (2012) 684–691.
- [4] T. F. Guiberti, D. Durox, T. Schuller, Flame chemiluminescence from CO₂- and N₂-diluted laminar CH₄/air premixed flames, *Combustion and Flame* 181 (2017) 110–122.
- [5] I. Schoegl, V. M. Sauer, P. Sharma, Predicting combustion characteristics in externally heated micro-tubes, *Combustion and Flame* 204 (2019) 33–48.
- [6] A. Di Stazio, C. Chauveau, G. Dayma, P. Dagaut, Combustion in micro-channels with a controlled temperature gradient, *Experimental Thermal and Fluid Science* 73 (2016) 79–86.
- [7] J. Kojima, Y. Ikeda, T. Nakajima, Basic aspects of OH(A), CH(A), and

- C2(d) chemiluminescence in the reaction zone of laminar methane-air premixed flames, *Combustion and Flame* 140 (1-2) (2005) 34–45.
- [8] T. S. Cheng, C. Y. Wu, Y. H. Li, Y. C. Chao, Chemiluminescence measurements of local equivalence ratio in a partially premixed flame, *Combustion Science and Technology* 178 (10-11) (2006) 1821–1841.
- [9] J. Yang, Z. Ma, Y. Zhang, Improved colour-modelled CH* and C2* measurement using a digital colour camera, *Measurement: Journal of the International Measurement Confederation* 141 (2019) 235–240.
- [10] J. Reyes, R. Kumar Abhinavam Kailasanathan, K. Ahmed, Relationship between the Chemiluminescence Intensity Ratio of C2* and CH*, Charge Pressure, and Equivalence Ratio for Gasoline, *Energy and Fuels* 32 (10) (2018) 10933–10940.
- [11] T. Clark, Studies of OH, CO, CH, and C2 Radiation from Laminar and Turbulent Propane-Air and Ethylene-Air Flames, Technical Note 4266; National Advisory Committee for Aeronautics, Washington, DC, USA (1958) 1–25.
- [12] Y. Ikeda, T. Kurahashi, N. Kawahara, E. Tomita, Temperature Measurements of Laminar Propane / Air Premixed Flame Using Detailed OH* Spectra Intensity Ratio, 12th International Symposium on Applications of Laser Techniques to Fluid Mechanics (1) (2004) 1–11.
- [13] Y. K. Jeong, C. H. Jeon, Y. J. Chang, Evaluation of the equivalence ratio of the reacting mixture using intensity ratio of chemiluminescence

in laminar partially premixed CH₄-air flames, *Experimental Thermal and Fluid Science* 30 (7) (2006) 663–673.